Study on the Thermal Behaviors and the Morphology in PVP and Nylon 6 Blends

Chaowei Hao,[1,2] Ying Zhao,[1] Dujin Wang,[1] Guoqiao Lai[2]

[1]*Beijing National Laboratory for Molecular Sciences, Key Laboratory of Engineering Plastics, Institute of Chemistry, Chinese Academy of Sciences, Beijing 100190, China*
[2]*Key Laboratory of Organosilicon Chemistry and Material Technology, Ministry of Education, Hangzhou Normal University, Hangzhou 310012, People's Republic of China*

Received 6 January 2011; accepted 8 March 2011
DOI 10.1002/app.34491
Published online 27 July 2011 in Wiley Online Library (wileyonlinelibrary.com).

ABSTRACT: In this report, polyamides were solution blended in the formic acid with poly(vinyl pyrrolidone)(PVP), an amorphous polar polyamide. The thermal behaviors and morphological change in the blends of Nylon 6 (PA6) and PVP were investigated in details via WAXD, DSC, FT-IR and POM methods. The equilibrium melting temperatures for PA6 in the blends were estimated based on the linear and nonlinear Hoffman-Weeks (LHW and NLHW) extrapolative methods. With increasing the mass ratio of PVP to PA6, T_m (melting temperature) and T_c (crystallization temperature) of PA6 in blends both decreased as well as that of the spherulite size of PA6. The interaction mode between PVP and PA6 was investigated by FT-IR spectroscopy, and the spectral changes indicated that the carbonyl groups of PVP had formed hydrogen bonding with the *N*—H groups of PA6 molecules in the molten state, which resulted in the variation of the morphology and thermal behaviors. © 2011 Wiley Periodicals, Inc. J Appl Polym Sci 123: 375–381, 2012

Key words: Nylon 6; equilibrium melting point; miscibility; infrared spectroscopy; spherulites

INTRODUCTION

Tremendous interests have been focused on the miscibility between polymers in the blends over the past 20 years both from scientific and engineering view points.[1] Generally, miscible polymer blends can be obtained via specific interactions such as dipole-dipole, hydrogen bonding, static interaction, and chemical reaction which act as driving forces for miscibility. Poly(*N*-vinyl-2-pyrrolidone) (PVP) is a water-soluble tertiary amide polymer, a proton acceptor polymer, which is always considered to be a strong Lewis base to compose with other Lewis acids polymers, such as poly(vinyl alcohol),[2–4] poly(*p*-vinyl phenol),[5] poly(hydroxyethyl methacrylate),[6] etc.

For miscible polymer blends, the research mostly focused on two aspects: multimelting behavior and polymeric spherulites studies. The study in the melting process of the crystalline or semicrystalline polymers, especially of the semicrystalline polymers (e.g., nylons), have been attractive for many scientists in the past half century accompanied with a large number of articles published.[7–12] However, the multiple melting behavior is still not be fully understood and there is no general consensus on its origin. The interpretation varies from different crystal structures[13] or lamellar thickness[14] to simultaneous melting and recrystallization.[15] At present, it is usually recognized that the multiendotherms arisen from several different factors which are dependent upon the sample properties and thermal history. Examples of the causes are different crystalline phases and recrystallization behavior during the DSC experiment. Whereas spherulites are produced for most of the crystalline polymers in an environment free of stress (mechanical or thermal disturbance). The studies on spherulites for crystalline or semicrystalline polymers (e.g., nylons) from the molten state in which an amorphous composition is introduced have been carried out for a long time.[16–20] Some formation mechanisms of the spherulite were proposed as well.

In summary, there are a few articles discussing multiple-melting behavior as well as the spherulite in the nylons' blends, but there is no general consensus on its origin. Furthermore, some formation mechanisms of the spherulite are proposed, but there is no convincing theory or explanation on them. In this article, summarizing a throughout

Correspondence to: C. Hao (cwhao@iccas.ac.cn).
Contract grant sponsor: National Natural Science Foundation of China; contract grant number: 50403026.
Contract grant sponsor: Major Science and Technology Projects of Science and Technology Department of Zhejiang Province; contract grant number: 2010C11043.

investigation carried out by our research group about the influence of PVP with different molecular weight on the thermal properties and morphology of PA6 spherulites in detail. And the possible interaction mechanism was proposed as well.

MATERIALS AND METHODS

Poly(vinyl pyrrolidone) (PVP) with molecular weights M_w = 40,000g/mol (PVPK30) and M_w = 1,300,000g/mol(PVPK90) were purchased from Sigma and Acros, respectively. PA6 pellet was purchased from Ba Ling Petrochemical Corp., Yueyang.

Films for wide angle X-ray diffraction (WAXS) were prepared by solution blending in formic acid with desired molar ratio followed by the solvent evaporated and dried at 100°C under vacuum overnight to eliminate the residual solvent. Then the samples were sandwiched between Teflon sheets and melt pressed in a hydraulics hot press under nitrogen atmosphere.

FT-IR spectra of all blends were recorded using a Bruker EQUINOX 55 FT-IR Spectrophotometer. All infrared spectra were obtained in the range 4000–400 cm^{-1} with a resolution of 4 cm^{-1} and scanning once per 5°C from 25 to 175°C under reduced pressure to avoid oxidation of the samples and the influence of moisture on the spectrum.

Differential Scanning Calorimetry experiments were performed on a Perkin–Elmer DSC-7. The measurements were conducted under a dry nitrogen flow rate of ca. 25 mL/min. PVP/PA6 samples were heated to 250°C, subsequently hold for 10 min, rapidly cooled to 50°C, and then reheated to 250°C at the rate of 10°C/min. The isothermal crystallization experiment was carried out as well.

Investigation on the spherulic morphology of polyamides was carried out on Leika POM. The samples for POM experiment were spread onto glass slides and dried under vacuum over night to completely remove the residual solvent. The samples of PA6 blends for POM were melted at 250°C for 3 min to eliminate the thermal history, then quenched to 190°C and annealed for 20 min. After that, the samples were observed under POM at room temperature.

RESULTS AND DISCUSSION

Wide angle X-ray diffraction

PA6 samples typically showed the triclinic structure described by Bunn and Garner.[21] Figure 1 showed the X-ray diffraction patterns of the PVP and polyamides blends. In pure PA6, PVPK90/PA6 and PVPK30/PA6 blends, two major peaks located at 2θ angles of 20° and 24° corresponding to the (100) and (010) spacings were almost the same. No other peaks in blends could be observed, and only with the intensity ratio of $I_{(010)}$ to $I_{(100)}$ increased as shown in curves a-e.

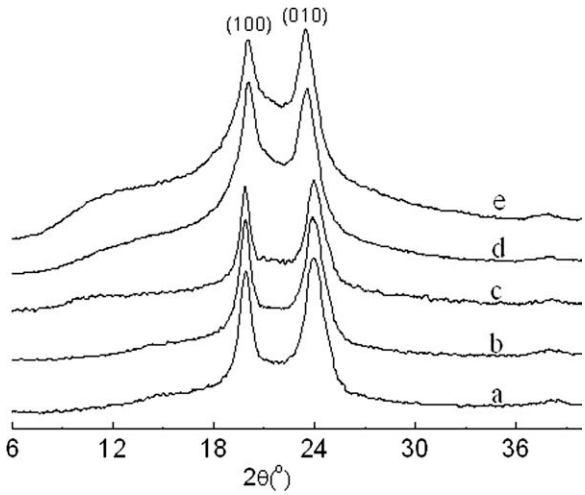

Figure 1 Wide angle X-ray diffraction patterns of solution-cast blends. a:PA6; b:PVPK90/PA6-20/80; c:PVPK90/PA6-50/50; d:PVPK30-20/80; e:PVP/K30/PA6-50/50.

Differential scanning calorimetry

Multimelting peak behavior and the equilibrium melting temperature of the PVPK90/PA6 and PVPK90/PA66 blends

Figure 2 showed DSC thermograms of PVP/PA6 blends which were melted at 250°C for 5 min, respectively, followed by rapid cooling to desired crystallization temperature (T_c) and holding for needed time, then reheating to 250°C, at the heating rate of 10°C/min. Melting behaviors of PA6 were characterized by the presence of three endothermic peaks: they were (1) the minor endothermic peak (located close to the corresponding crystallization temperature T_c, namely peak I(left)), (2) the low-temperature melting endothermic peak [namely peak II (middle)] and (3) the high-temperature melting endothermic peak [namely peak III (right)].

Figure 3 gave plots of the minor peak temperature T_{m1}, the low-melting peak temperature T_{m2} and the high-melting peak temperature T_{m3} as a function of the isothermal crystallization temperature T_c. T_{m1} increased linearly with the crystallization temperature, which was parallel to the $T_m = T_c$ line. This indicated that melting behavior of peak I always started at a temperature closed to the crystallization temperature, which implied that the minor Peak T_{m1} was corresponding to the temperature when the imperfect crystalline phase (secondary crystallization) formed between the primary crystallization lamella began to melt. And the low-melting peak T_{m2} was related to the melting of the primary

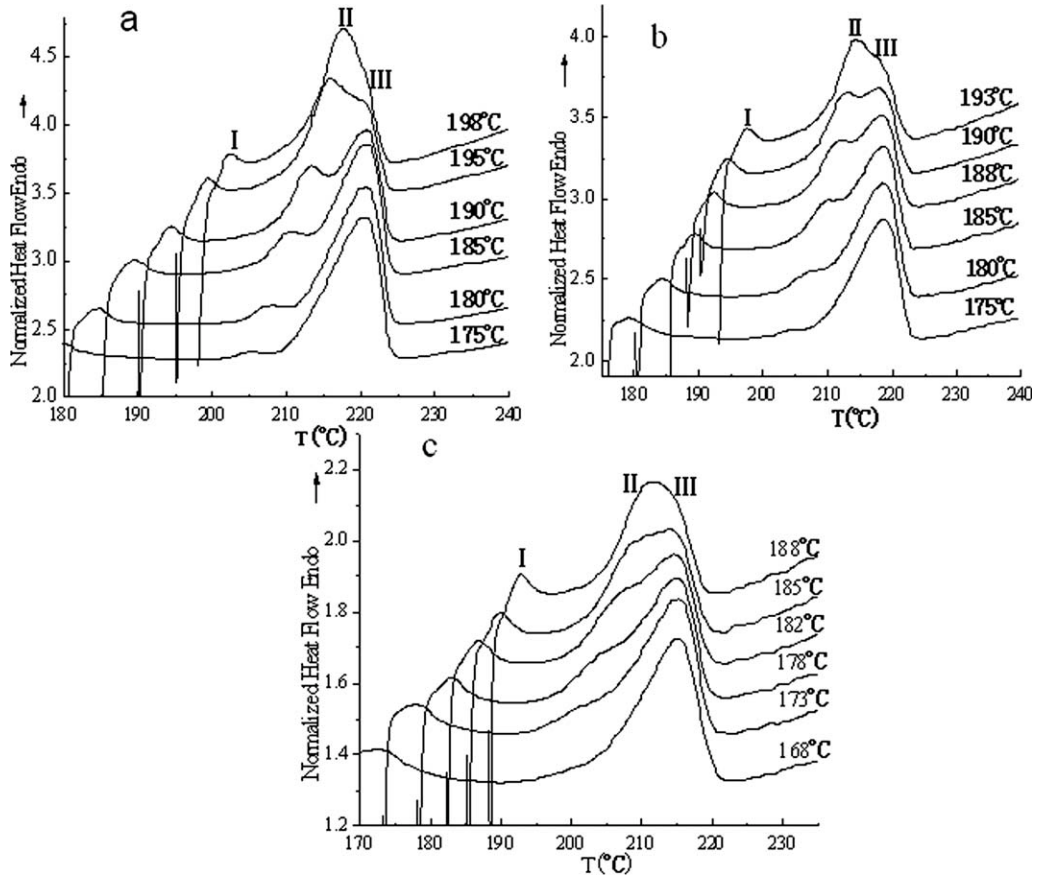

Figure 2 DSC thermograms of K90/PA6 films solution-cast at depressed pressure: a: PA6; b: K90/PA6-20/80; c: K90/PA6-50/50.

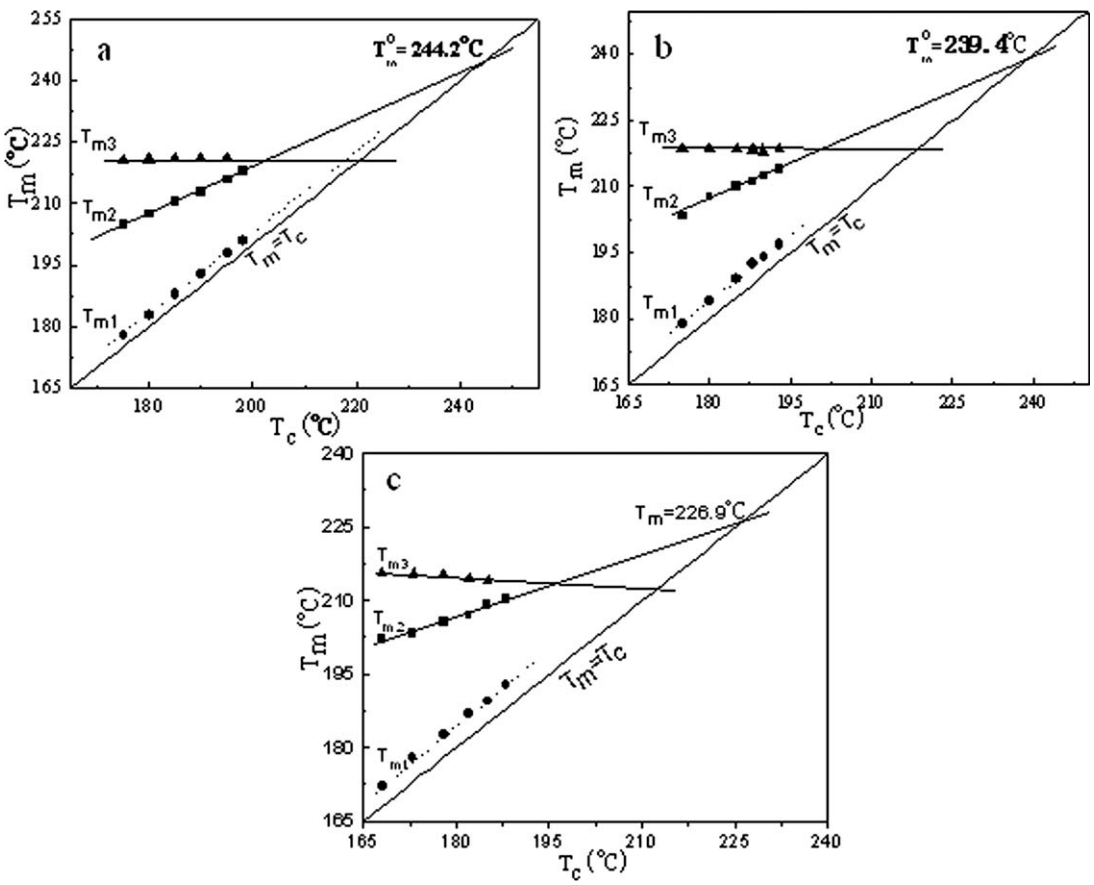

Figure 3 The identity of the equilibrium melting temperature from DSC thermograms of K90/PA6 films solution-cast at depressed pressure: a: PA6; b: K90/PA6-20/80; c: K90/PA6-50/50

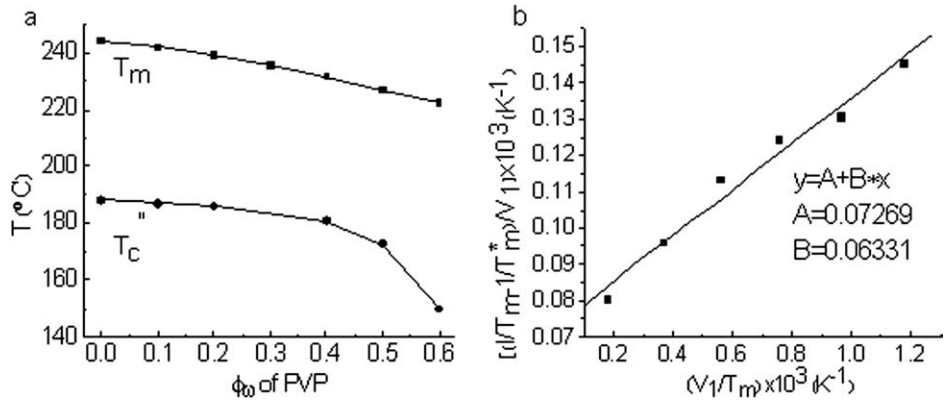

Figure 4 The equilibrium melting temperature and crystal temperature from DSC thermograms of K90/PA6 films as function of the weight fraction of PVPK90 (a), and the volume fraction based on the Nishi W. equation (b). The solid curve is theoretical value, and the dot is experimental results shown in Figure 4b.

crystallization formed at isothermal crystallization temperature T_c. At last, the high-melting peak T_{m3} was attributed to the melting of the recrystallization crystallites during the heating process.

The equilibrium melting temperatures T_m^0 of the different samples were determined by so-called Hoffman's T_m-T_c extrapolation.[22] As shown in Figure 3, the temperatures of Peak I were always higher $\sim$ 4°C than the crystallization temperature (T_c) and the temperatures of Peak III were almost constant regardless of T_c, which indicated that they were not melting temperatures of the primary crystallization of PA6 under the given experimental conditions. Therefore both Peaks I and III were useless in determination of T_m^0 of the PVPK90/PA6 blends. And Peak II were used to determine the T_m^0 since it increased linearly with T_c.

Figure 4(a) showed how the equilibrium melting temperature and the crystallization temperature (T_c'') of the PVPK90/PA6 blends depended on the weight fraction of PVPK90 in the blends. It was clearly suggested that the melting points depressed gradually with the amorphous PVPK90 content increasing. The melting point decreasing phenomenon was similar to the one observed in the crystalline polymer-diluent systems. Several mechanisms had been proposed regarding the melting point depression in the latter systems[23,24] and it had been suggested morphological effects such as size and the perfection of the crystalline regions were responsible for the lowering of melting point of PA6.

A possible explanation for the observed melting point decreasing phenomenon was to consider the thermodynamic effects of mixing by extending the work on the crystalline polymer-diluent systems[23] to the crystalline polymer-amorphous polymers systems. As argued by Scott[25] using the Flory-Huggins approximation,[24] the thermodynamic mixing of two polymers was treated. For the given system the chemical potential $\mu_{2u}{}^1$ per mole of crystallizable polymer units in the mixing relative to its chemical potential μ_{2u}^0 in the pure liquid could be expressed as

$$\mu_{2u^1}-\mu_{2u^0}=\frac{TRV_{2u}}{V_{1u}}\left[\frac{\ln V_2}{m_2}+\left(\frac{1}{m_2}-\frac{1}{m_1}\right)\times(1-V_2)+\chi_{12}(1-V_2)^2\right] \quad (1)$$

where, the subscript 1 identified with amorphous polymers and 2 with the crystalline polymer, V was the volume fraction, V_u was the molar fraction of the repeating units, m was essentially the polymerization degree.[26] And the χ_{12} was the polymer–polymer interaction parameter, R was the gas constant, and the T was the absolute temperature.

Considering the correlation of the chemical potential, the enthalpy and the entropy of the fusion of the crystal polymer, and by means of a series of thermodynamic approximation and mathematic treatment, the following equation was finally gained:

$$\frac{1}{V_1}\left[\frac{1}{T_m}-\frac{1}{T_m^0}\right]=-\frac{\beta V_{2u}}{\Delta H_{2u}}\times\frac{V_1}{T_m} \quad (2)$$

where β was the interaction energy density characteristic of the polymer pair and ΔH_{2u} was the enthalpy of fusion per mole of repeating unit of crystalline polymer. Scott's equation provided a direct determination of the interaction parameter between a crystallizable polymer and an amorphous polymer.

It was shown that the relationship between $(1/V_1)\times[(1/T_m)-(1/T_m^0)]$ and V_1/T_m was linear. And the data obtained in Table I was plotted with $(1/V_1)\times[(1/T_m)-(1/T_m^0)]$ versus V_1/T_m, as shown in Figure 4(b). Calculation showed a value, A, of $7.3\times10^{-5}K^{-1}$ for the ordinate of the intersection point and 6.331×10^{-2} for the slop B. Connected the values of the density, volume and the molar enthalpy

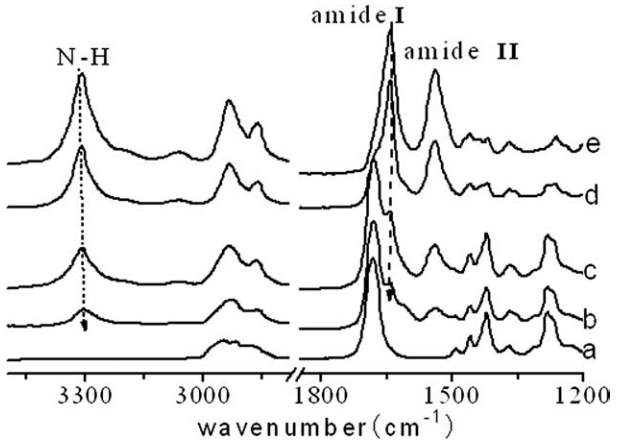

Figure 5 IR spectra of the PVPK90/PA6 blends under reduced pressure at 175°C in the range of 1200∼ 3450cm^{-1}. The component of the PVPK90/PA 6 blends are, a: 100/0, b: 90/10, c: 50/50, d: 10/90, e: 0/100.

of the PVP and PA6, the following parameters could be obtained:

$$\beta = -13.52\text{J/cm}^3(\text{of PVPK90}), \chi_{12} = -0.302 \text{ at } 220^\circ\text{C}$$

χ_{12} of PVPK90/PA6 system was less than zero, which indicated that the polymer pair could formed a thermodynamically stable compatible mixture at temperature above the melting point of PA6.

FT-IR spectroscopy

Fourier Transform Infrared (FT-IR) spectroscopy was extensively used to the characterize polymer blends. Information about the nature, strength, and number of intermolecular interactions among the components as a function of temperature had been obtained. Extensive research on hydrogen bonding in polyamides and polyurethanes had been performed by several authors.[27–30] Figure 5 showed the infrared spectra of the PVPK90/PA6 blends casting onto a KBr window recorded at 175°C under reduced pressure in the range 1200 –3450 cm^{-1}. For expository convenience, we would separately describe the results obtained in two major spectral regions.

N-H stretching band

Generally, the *N*—H stretching band of polyamides covered a range of 3100–3450 cm^{-1}. The *N*—H stretching band ν_{N-H} located at 3312 cm^{-1} for pure PA6, and shifted to lower wave number upon the addition of PVPK90, until to 3302 cm^{-1} for the PVPK90/PA6(90/10) blend film, and the half-peak width of ν_{N-H} was broadened obviously, which indicated that several *N*—H bonding states existed in the blends. The above variations suggested that the hydrogen bonding between PA6 molecules had been partially destroyed by the PVPK90 molecules due to formation of new hydrogen bonding between the carbonyl groups of PVP molecules and the *N*—H groups of PA6 molecules, and the strength of new hydrogen bonding might be stronger, which accounted for the red shift of ν_{N-H} of PA6 molecules.

Amide I band

Unlike the isolated *N*—H stretching vibrations, the amide I band exhibited more complex vibrations. The amide I band could be ascribed to the C=O stretching, the C—N stretching, and the C—C—N deformation vibrations.[25] The stretching vibration $\nu_{C=O}$ of PVP locates at 1682 cm^{-1} was overlapped with the amide I band of PA6. As shown in Figure 5, the stretching vibration of C=O of the PVPK90/PA6 blends clearly exhibited two peaks, and the $\nu_{C=O}$ band of PVP shifted to lower wave number and the one of PA6 changes inversely and accompanied the peak broadening.

Figure 6 showed the curve fitting results of PVPK90/PA6 with molar ratio 50/50 (a), 80/20 (b). Three peaks were obtained in both Figure 6(a,b), exhibiting differences in the peak area and the peak

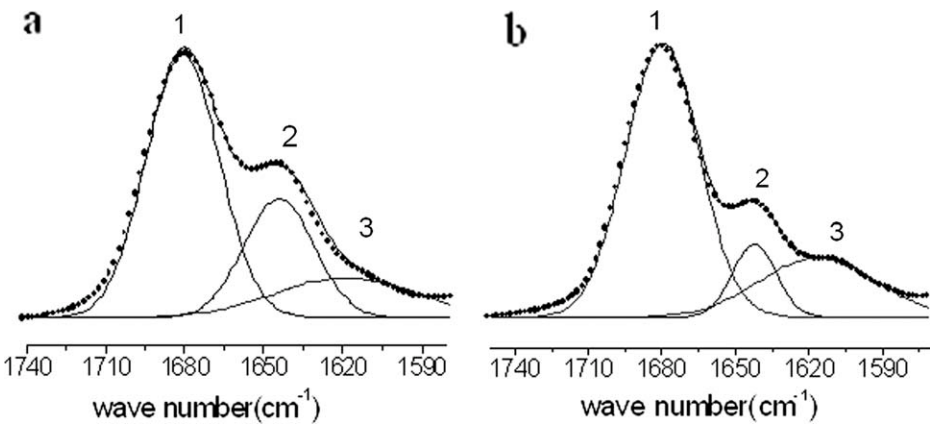

Figure 6 The curve fitting results of PVPK90/PA6-50/50(a) and PVPK90/PA6-80/20(b) blends.

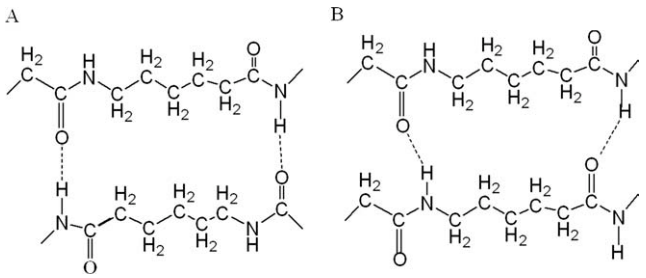

Figure 7 The hydrogen bond arrangement in PA6 crystal zone. A: all hydrogen bonds made perfectly by inverting alternate chains; B: all hydrogen bonds made imperfectly.

position in the two blends. With addition of PVP, the peak area of 1615 cm^{-1} band increased obviously. The appearance of new peak(I) at 1615 cm^{-1} indicated that there was new state of carbonyl group in the blend, which was consistent with the variation of ν_{N-H} that partial hydrogen bonding between the PA6 molecules were destroyed due to the interaction between carbonyl groups of PVP with the *N*—H group of PA6. Combined with the variation of ν_{N-H} band, $\nu_{C=O}$ of PA6 should shift to higher wavenumber and overlap with the $\nu_{C=O}$ band of the PVP, which accounted for the larger peak intensity for the peak located at ca. 1680 cm^{-1} and the smaller peak intensity corresponding to the carbonyl group

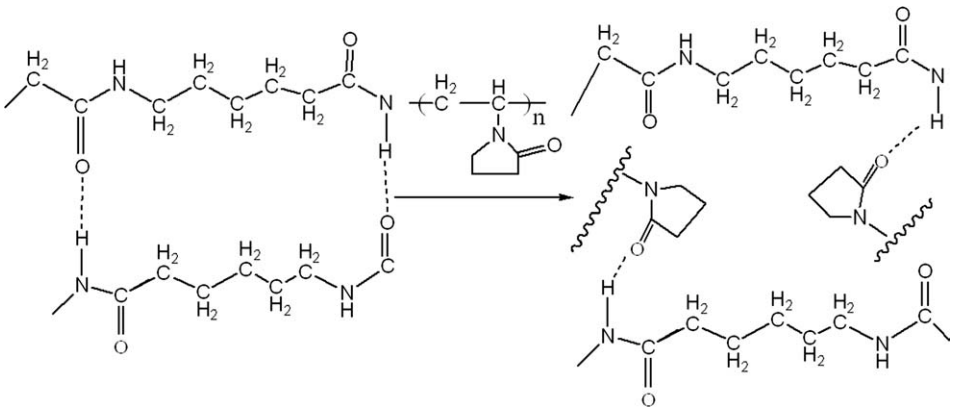

Figure 8 The schematic plan of the hydrogen bonds in crystal zone of the PA 6 destroyed by PVP.

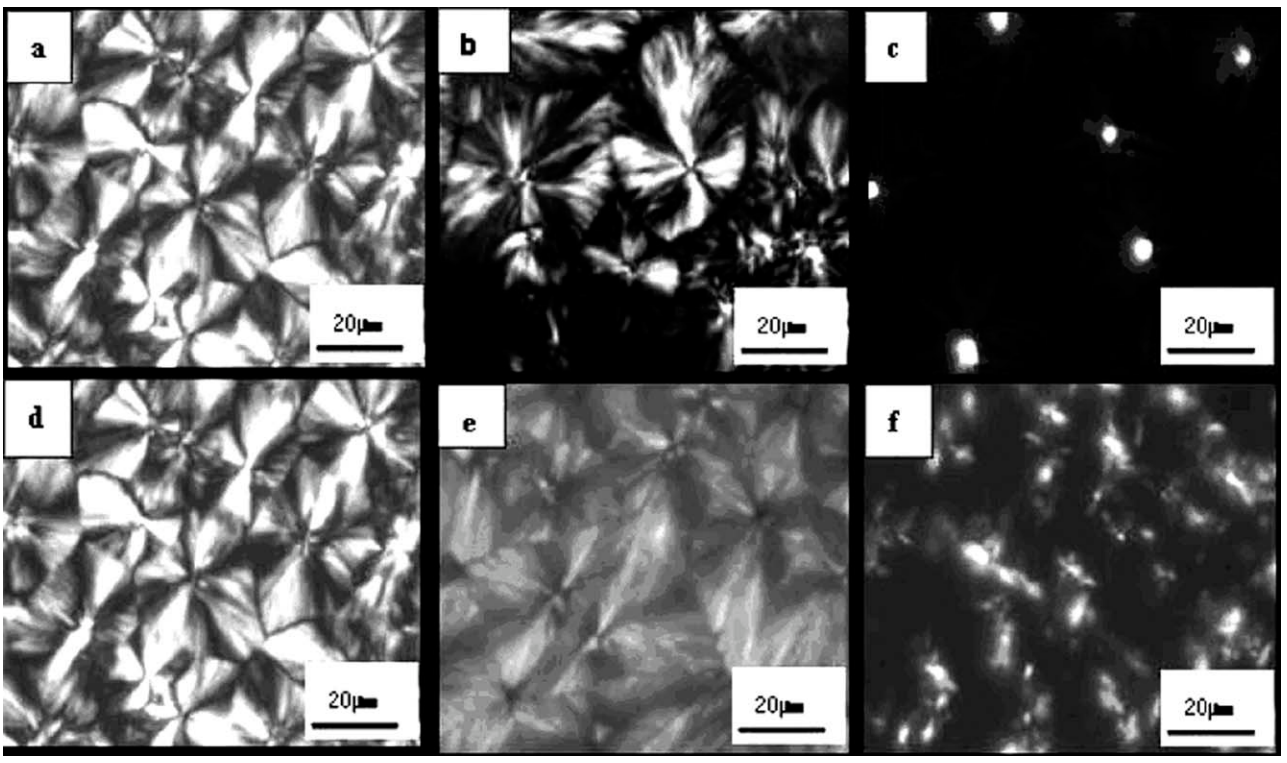

Figure 9 The spherulitic crystal morphologies of PA6 in PVPK90/PA6 blends reflected by the POM: a: 0/100; b: 50/50 c: 80/20; PVPK30/PA6 blends reflected by the POM: d: 0/100; e: 50/50; f: 80/20. The ratio is calculated by mass fraction.

absorption in the hydrogen sheet of the PA6 molecules. Accompanied the formation of the new hydrogen bond between the *N*—H group in PA6 molecules and the C=O group in PVP molecules, the $\nu_{C=O}$ of the PVP molecules clearly shifted to lower frequency and the peak intensity became stronger in Figure 6(b) compared with that of the $\nu_{C=O}$ in Figure 6(a).

According to Ref. 31 the hydrogen bonding in PA6 had two forms: perfect and imperfect arrangements. Combined with the above IR spectral results, and the interaction mode between PA6 and PVP molecule in the molten state was speculated showing in Figures 7 and 8, respectively.

POM experiment

Optical studies were carried out on pure PA6 and their blending with PVP using polarized microscopy. After the thermal treatment with hot stage under nitrogen atmosphere, the spherulites with different morphology were obtained. When PVP molecules were introduced into PA6 matrix, the morphology and the size of the spherulites changed correspondingly, which was the most notable effect of PVP as a diluent in suppressing the primary nucleation of spherulites.

Figure 9 gave the spherulitic morphology of the PVPK90/PA6 (a–c) and PVPK30/PA6 (d–f) blends. The addition of 10% PVPK90 led to the decrease of the spherulitic size of PA6. Imperfect spherulites were obtained when the PVPK90 content reached 50%, and the spherulite disappeared with 80% PVP addition to. Whereas compared with that of PVPK90/PA6 systems, small difference existed in PVPK30/PA6 blends. When lower content (10%) of PVPK30 was added to PA6, there were little influence on the spherulites of PA6. And when PVPK30 content reached 50%, the spherulites became irregular and the spherulitic size decreased, which indicated that there were obvious interactions between PA6 and PVP. A clear difference existed between the PVPK90/PA6 and PVPK30/PA6 systems with the PVP content being 80%, as shown in Figure 9, no spherulites could be observed for PVPK90/PA6, while imperfect spherulites still could be observed in PVPK30/PA6 system. The reason for this difference might be related to the difference of the viscosity or the molecular mobility of these two PVP molecules. For PVPK30, the smaller molecular weight mean less entanglement and better molecular mobility, compared with that of PVPK90, which was inclined to induce the formation of microphase-separation more easily. The better mobility for PA6 molecules, the easier being repelled out of the crystal lattice for PVP chains during the crystallizing process for PA6. Therefore, spherulites still clearly existed when the PVPK30 content reached 80% in PVPK30/PA6 system and disappeared for PVPK90/PA6 blend.

CONCLUSIONS

The blends of PA6 with PVPK30 and PVPK90 prepared by solution casting were characterized via X-ray, DSC, FT-IR and POM techniques in details. It was showed that the PVP molecular weight had little influence on the crystalline phase of PA6. But the thermal behaviors of the blends, such as the melting point depression, multiple melting behaviors, etc. were much influenced by introducing the PVP component into PA6 matrix. FT-IR results showed that the hydrogen bonding between PA6 molecules had been partially destroyed by PVP molecules due to formation of new stronger hydrogen bonding between the carbonyl groups of PVP molecules and the *N*—H groups of PA6 molecules, which accounted for the obviously thermal behavior change in the blends. Furthermore, the spherulitic morphology of PA6 was tightly dependent on the molecular weight of PVP as well.

References

1. Walsh, D. J.; Rostami, S. Adv Polym Sci 1985, 70, 119.
2. Ping, Z. H.; Nguyen, Q. T.; Neel, J. Makromol Chem 1989, 190, 437.
3. Thyagarajian, G.; Janarthanan, V. Polymer, 1989, 30, 1797.
4. Zhang, H.; Yin, J. Makromol Chem 1990, 191, 375.
5. Moskala, E. J.; Varnell, D. F.; Coleman, M. M. Polymer, 1985, 26, 228.
6. Goh, S. H.; Siow, K. S. Polym Bull 1990, 23, 205.
7. Bell, J. P.; Slade, P. E.; Dumbleton, J. H. J Polym Sci A-2 1968, 6, 1773.
8. Hybart, F. J.; Platt, J. D. J Appl Polym Sci, 1967, 11, 1449.
9. Bell, J. P.; Dumbleton, J. H. J Polym Sci A-2 1969, 7, 1033.
10. Ishikawa, T.; Nagai, S. J. Polym Sci: Polym Phys Edit 1980, 18, 1413.
11. White, T. R. Nature 1953, 175, 895.
12. Ramesh, C.; Keller, A.; Eltink, S. J. E. A. Polymer 1994, 35, 5300.
13. Ishikawa, T.; Nagai, S. J Polym Sci Polym Phys Ed 1980, 18, 1843.
14. Ko, T. Y.; Woo, E. M. Polymer 1996, 37, 116.
15. Lee, Y.; Porter, R. S.; Lin, J. S. Macromolecules, 1989, 22, 1754.
16. Lorenzo, M. L. D. Macromol Symp 2006, 234, 176.
17. Kyu, T.; Chiu, H. W.; Guenthner, A. J. Phys Rew Lett 1999, 83, 2749.
18. Ren, M. Q.; Mo, Z. S. Polymer 2004, 45, 3511.
19. Zhu, C. S.; Li, X. D.; Li, H. G.; Pu, S. T. Chem J Chin Univ 1991, 12, 1677.
20. Clark, C. L.; Kander, R. G.; Srinivas, S. Polymer 1998, 39, 507.
21. Bunn, C. W.; Garner, E. V. Proc Roy Sco Lond A 1947, 189, 39.
22. Lauritzen, J. I., Jr.; Hoffman, J. D. J Res NBS A 1960, 64, 73.
23. Mandelkern, L. Crystallization of Polymers; McGraw-Hill: NewYork, NY, 1964.
24. Flory, P. J. Principles of Polymer Chemistry; Cornell University Press: Ithaca, NY, 1953.
25. Skrovanek, D. J.; Howe, S. E.; Painter, P. C. Macromolecules 1988, 18, 1676.
26. Scott, R. L. J Chem Phys 1949, 17, 279.
27. Seymour, R. W.; Cooper, S. L. Macromolecules 1973, 6, 48.
28. Sung, C. S. P.; Schneider, N. S. Macromolecules, 1977, 10, 452.
29. Sung, C. S. P.; Schneider, N. S. Macromolecules 1975, 8, 68.
30. Senich, G. A.; MacKnight, W. J. Macromolecules 1980, 13, 106.
31. Holmes, D. R.; Bunn, C. W.; Smith, D. J. J Polym Sci 1955, 17, 159.